Composite Structures 200 (2018) 340–345

Contents lists available at ScienceDirect

Composite Structures

journal homepage: www.elsevier.com/locate/compstruct

Effect of dents in laminated carbon composite beams on modified anisotropic electric potential analysis

Akira Todoroki[a,*], Takuya Yamane[b]

[a] Tokyo Institute of Technology, 2-12-1, Oookayama, Meguro, Tokyo 1528500, Japan
[b] Tokyo Institute of Technology, Tokyo Institute of Technology, 2-12-1, Oookayama, Meguro, Tokyo 1528500, Japan

ARTICLE INFO

Keywords:
Laminated composites
Carbon
Electric current
Dent

ABSTRACT

Because carbon fiber reinforced polymer (CFRP) laminated composites have electric conductivity, damage monitoring was performed using electrical resistance changes. The authors previously proposed an anisotropic electric-potential function method to calculate the electric-potential field of laminated CFRP composites. The method, however, did not deal with the effects of dents. The present study deals with the effects of dents on the anisotropic electric-potential function method. The dent causes an electric conductivity increase in the through-thickness direction. The increase was modeled and applied to a beam-type specimen. The results were compared with the finite-element method results, and the method using equivalent conductivity in the through-thickness direction was confirmed to be effective.

1. Introduction

Carbon fiber reinforced polymer (CFRP) laminated composites are widely used for aerospace structures and automobile components. For CFRP laminates, it is difficult to detect defects visually. Carbon fibers have electrical conductivity. When CFRP laminates are damaged, the damage results in carbon fiber breakage and fiber contact cuts. These cause electrical resistance changes. Therefore, measuring electrical resistance makes it possible to monitor damage to CFRP laminates [1–14].

When a CFRP laminate is subjected to a load in the through-thickness direction, a dent is generated on the surface of the CFRP laminate. The dent causes plastic deformation of resin in the through-thickness direction, and this brings fiber contact in the though-thickness direction. The increase of contact causes a significant increase in electrical conductivity in the through-thickness direction [15]. In-plane shear loading is a well-known cause of plastic deformation, and this shear plastic deformation has been reported to increase electrical conductivity in the through-thickness direction [16]. The significant increase of conductivity in the thickness direction is equal to the significant increase of cross sectional area for electric current. This effect, therefore, is very important when plastic deformation occurs for CFRP laminates.

Todoroki et al. showed a new analytical method to calculate the electric current density and electric voltage change at the surface of the CFRP laminate using anisotropic electric potential analysis [17,18]. Yamane et al. experimentally showed the effectiveness of the method [19], and the method was extended to practical CFRP laminates that include angle plies [20]. Matsuzaki et al. showed that it is possible to identify multiple delamination cracks from the measurement of the surface electric potential using the analysis method [21]. Although the anisotropic electric potential function can be applied to the damage monitoring of the CFRP laminate, there was no approach to estimate the effect of a dent caused by out-of-plane loading, such as impact loads.

In this study, therefore, the anisotropic electric potential function is extended to calculate the effect of a dent that caused a local increase in the electrical conductivity in the through-thickness direction. The calculated results are compared with the finite-element method (FEM) results. As shown in [19,20], the effectiveness of the anisotropic electric potential function has been demonstrated experimentally, and the results agreed well with the FEM results. In the present study, therefore, the calculated results are compared with FEM results. The FEM results depend on mesh division. Three-dimensional FEM requires several mesh divisions to obtain reliable results. Here, two-dimensional analysis is performed using a beam-type specimen configuration. Moreover, a comparison of electric current distributions between a specimen without a dent and one with a dent is performed to confirm the effect of a dent.

* Corresponding author.
E-mail address: todoroki.a.aa@m.titech.ac.jp (A. Todoroki).

https://doi.org/10.1016/j.compstruct.2018.05.154
Received 2 February 2018; Received in revised form 22 May 2018; Accepted 30 May 2018
Available online 31 May 2018

2. Dent analysis using equivalent electric conductivity in the through-thickness direction

2.1. Unidirectional laminate

Let us consider the two-dimensional model. The horizontal x-axis is defined as the fiber direction, and the perpendicular z-axis is defined as to the through-thickness direction. The electric current density of i_x and i_z can be expressed with electric potential ϕ and conductivity σ_x and σ_z as follows.

$$i_x = -\sigma_x \frac{\partial \phi}{\partial x}, \quad i_z = -\sigma_z \frac{\partial \phi}{\partial z} \tag{1}$$

From the equation of continuity of electricity, the following equation is obtained.

$$\sigma_x \frac{\partial^2 \phi}{\partial x^2} + \sigma_z \frac{\partial^2 \phi}{\partial z^2} = 0 \tag{2}$$

The coordinate transformation to the isotropic space shown below is adopted.

$$\xi = \frac{x}{\sqrt{\sigma_x}}, \quad \zeta = \frac{z}{\sqrt{\sigma_z}} \tag{3}$$

Using this coordinate transformation, Eq. (2) changes to the following:

$$\frac{\partial^2 \phi}{\partial \xi^2} + \frac{\partial^2 \phi}{\partial \zeta^2} = 0 \tag{4}$$

Consider the current applying locates $(-a, 0)$ and the ground locates $(a, 0)$ as the source and sink points, respectively, in potential flow analysis. Let the applied total electric current be I to the two-dimensional beam shown in Fig. 1. The anisotropic electric potential function is given as follows [17]:

$$\phi = -\frac{I}{2\pi\sqrt{\sigma_x \sigma_z}} \ln \frac{\frac{(x+a)^2}{\sigma_x} + \frac{z^2}{\sigma_z}}{\frac{(x-a)^2}{\sigma_x} + \frac{z^2}{\sigma_z}} \tag{5}$$

Substituting Eq. (5) into Eq. (1) with the electric conductivity of fiber direction σ_0 $(=\sigma_x)$ and the conductivity of the through-thickness direction σ_t $(=\sigma_z)$ gives the electric current density. When the laminate includes angle plies, the modification is shown in [20].

2.2. Analysis of effect of dent

As mentioned in Section 2.1, let us consider the case where the fiber direction is along the x-axis (horizontal direction) and the through-thickness direction is the z direction of the unidirectional beam-type specimen, as shown in Fig. 1. In [15], the experimental results for dents showed a local decrease in cross-sectional area and a significant increase in the electric conductivity in the through-thickness direction.

Even for a large dent, the decrease of thickness was only 1%, and the decrease comes from the plastic deformation of the epoxy resin. Because the epoxy resin is an electric insulator, the decrease of thickness has a negligible effect on the electrical resistance of the specimen, because the plastic deformation of the resin has little effect on the electric current path. As shown in [15], the dent causes an increase in the fiber volume fraction, and this causes an increase in electric conductivity in the through-thickness direction. This study addresses the local increase in conductivity in the through-thickness direction.

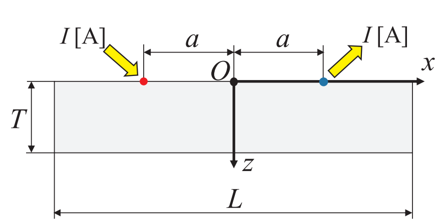

Fig. 1. Schematic representation of unidirectional CFRP laminate with electric current source and sink points.

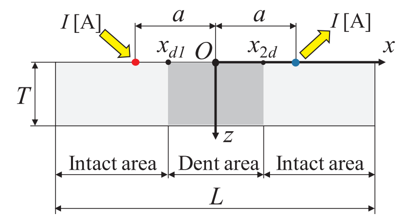

Fig. 2. Schematic representation of the laminate with dent at the area $x_{1d} \le x \le x_{2d}$ throughout the thickness.

The present modification assumes that the dent is equal to the local electric conductivity increase in the through-thickness direction, as shown in Fig. 2. The decrease in the thickness is neglected. In the present study, as shown in Fig. 2, a dent area is located from $x_{1d} \le x \le x_{2d}$, almost at the center of the beam-type specimen. The dent area has higher electric conductivity in the through-thickness direction, but the electric conductivity in the fiber direction is the same as that of the intact area. This means that σ_z in Eq. (3) varies depending on x.

Let us assume that the anisotropic electric potential function is differentiable, even if the beam has a dent. Because the anisotropic electric conductivity in the through-thickness direction is not uniform in the entire specimen, the anisotropic electric potential with a dent is different from that without a dent. To express this difference, an equivalent electric conductivity is adopted here. This means the function is assumed to be Eq. (5), but the electric conductivity in the through-thickness direction is different from the unidirectional CFRP beam.

As σ_z differs depending on the x coordinate, we define a new contribution function F_z that expresses the contribution of the local dent area. The contribution function F_z is defined as follows.

$$F_z(\beta) = \frac{\left.\frac{\partial \phi}{\partial z}\right|_{\substack{x=\beta L \\ z=t}}}{\max \left.\frac{\partial \phi}{\partial z}\right|_{z=t}} \tag{6}$$

where t is an arbitrary location of the z coordinate within the beam specimen, and β is the normalized location in the x coordinate $(-1/2 \le \beta \le 1/2)$. The denominator of Eq. (6) means the maximum value of the partial differential of ϕ with respect to z at the depth $z = t$. Using the normalized contribution function F_z, the equivalent electric conductivity is defined as follows.

$$C_z = \frac{\int_{-1/2}^{1/2} \sigma_z F_z(\beta) d\beta}{\int_{-1/2}^{1/2} F_z(\beta) d\beta} \tag{7}$$

To calculate the equivalent conductivity in the through-thickness direction C_z, iterative calculations are required using Eq. (7).

1. Calculate the contribution function F_z using Eq. (6), substituting σ_0 and σ_t with σ_x and σ_z, respectively.
2. Using the calculated contribution function F_z, calculate the equivalent electric conductivity C_z using Eq. (7).
3. Calculate the contribution function F_z again, using Eq. (6) and substituting σ_0 and C_z with σ_x and σ_z, respectively.
4. Using the calculated contribution function F_z, calculate the equivalent electric conductivity C_z again, using Eq. (7).
5. Perform steps 3 and 4 repeatedly until convergence is obtained. (In the present study, the threshold value is set to 10^{-2} of σ_t.)
6. Use the converged value as the equivalent electric conductivity.

Using the obtained equivalent conductivity in the through-thickness

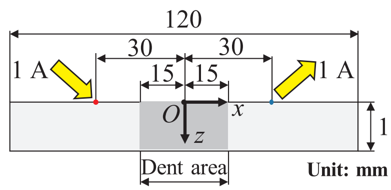

Fig. 3. Schematic representation of the analysis model of the laminate with dents with the area $-15\,\text{mm} \le x \le 15\,\text{mm}$ throughout the thickness.

direction C_z and the electric conductivity of fiber direction σ_0, we can calculate electric current density with Eq. (1). When a cross-ply laminate has a dent, not only the electric conductivity of the through-thickness direction C_z but also the electric conductivity in the x direction C_x must be exchanged with the equivalent electric conductivity, as described in [20].

3. Comparison with FEM results and discussion

3.1. Analytical model

In this study, two types of stacking sequences of the specimens are selected for the analyses: unidirectional and cross-ply $[0/90]_S$. The analysis model is a beam-type two-dimensional model, as shown in Fig. 3. The applied electric current is 1 A. For the electric current density analyses, only the conductivity ratio is important. The conductivity in the fiber direction is set to 1 S/m, and two conductivity ratios $\gamma = \sigma_0/\sigma_t = 100$ and 10,000 are used for the calculations. The conductivity of the 90° ply is fixed at $\sigma_{90} = 0.1$ S/m.

To model the increase in the electric conductivity in the through-thickness direction in the dent area, the electric conductivity in the through-thickness direction is considered 10 times larger than that of the normal intact area. The thickness of one ply is 0.25 mm. The dent area is on the center of the beam-type specimen from -15 mm to 15 mm. As mentioned before, the decrease in thickness is neglected here.

For each stacking sequence, three distributions of electric current density are calculated: distributions of i_x at $x = 0$ with respect to the z axis, distributions of i_z at $z = 0.1$ mm, and distributions of i_z at $z = 0.5$ mm. To obtain the equivalent conductivity C_z in Eq. (6), $t = 0.5$ mm is substituted in the equation. Mirror images are indispensable for this analysis of the finite boundary specimens, so 100 mirror images are placed in the x and z direction [19].

Commercially available FEM software ANSYS v.16.1 was used to obtain FEM results for comparison. For the FEM analyses, square elements were used. For the case of $\gamma = 100$, an element of 0.1 mm (length) × 0.01 mm (depth) was adopted. For the case of $\gamma = 10{,}000$, an element of 0.1 mm (length) × 0.001 mm (depth) was used. These element dimensions were decided to obtain converged results by downsizing the dimensions of the elements.

3.2. Unidirectional specimen

Fig. 4 shows the comparison results of $\gamma = \sigma_0/\sigma_t = 100$ of the unidirectional specimen. Fig. 4(a) shows i_x (electric current density in the x direction): the abscissa is the z coordinate, and the ordinate is i_x at $x = 0$. Fig. 4(b) shows i_z (electric current density in the z direction): the abscissa is the x coordinate, and the ordinate is i_z at $z = 0.1$ mm.

For the unidirectional laminate, we do not need to calculate the equivalent conductivity in the x direction. In Eq. (2), therefore, $\sigma_x = 1$ [S/mm] was used for the calculation, and $C_z = 0.0112$ was obtained as the equivalent conductivity in the z direction described in Section 2.2.

Fig. 4(c) shows i_z: the abscissa is the x coordinate, and the ordinate is i_z at $z = 0.5$ mm. The solid curves are the FEM results, and the open square symbols are the results of the analysis of this study. These figures show that the calculated results agree well with the FEM results. As shown in Fig. 4(c), i_z at $x = 0.5$ mm has a discontinuous distribution at the local dent area ($-15\,\text{mm} \le x \le 15\,\text{mm}$). The anisotropic electric potential function using the new equivalent conductivity successfully models the effect of a dent.

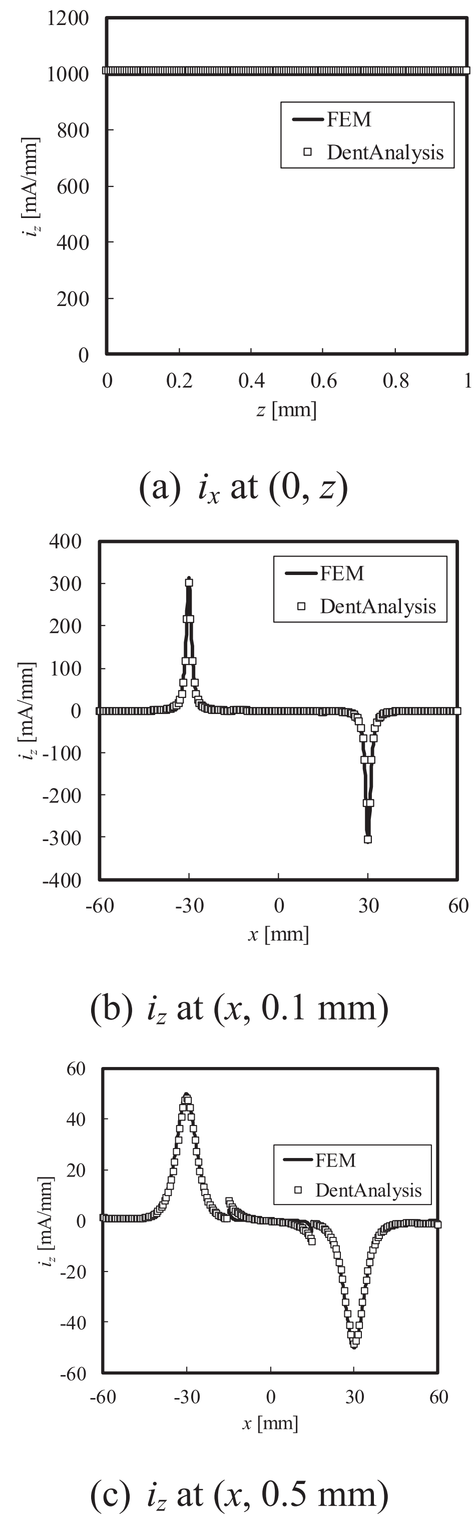

Fig. 4. Electric current density obtained by FEM and proposed dent analysis method for unidirectional laminates whose ratio of electric conductivity in each direction is 100.

Fig. 5 shows the comparison results of $\gamma = \sigma_0/\sigma_t = 10{,}000$ for the unidirectional specimen. Fig. 5(a) shows i_x (electric current density in

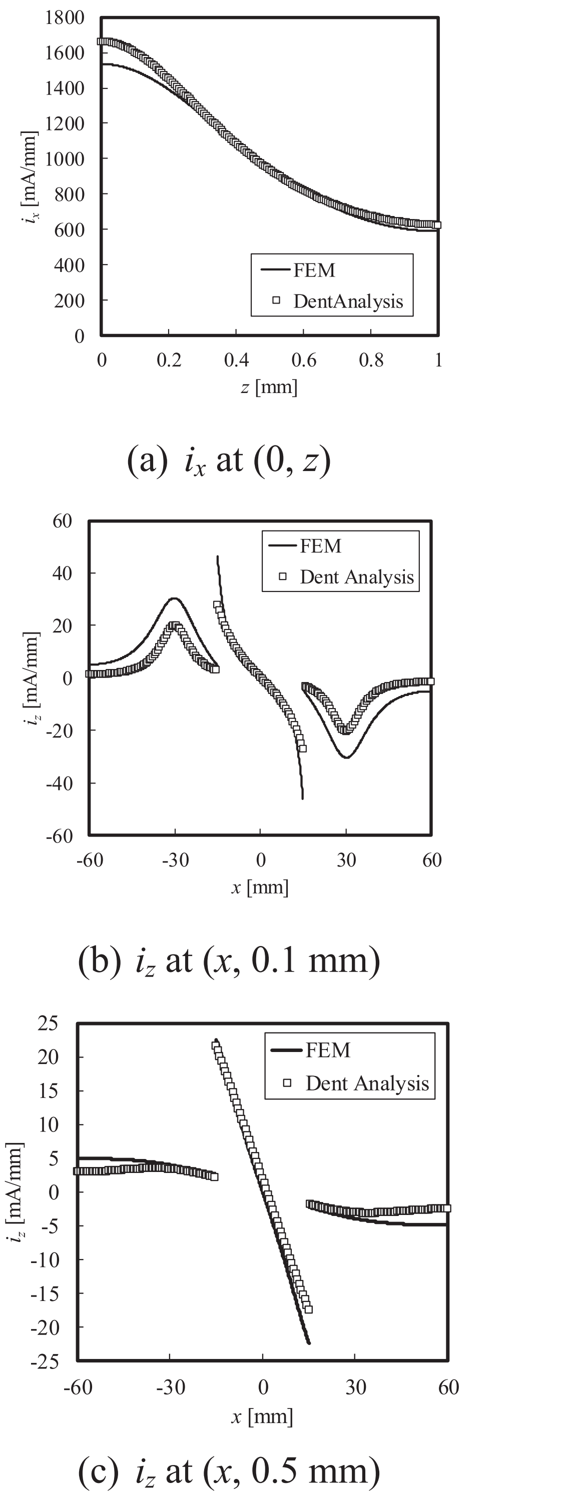

Fig. 5. Electric current density obtained by FEM and proposed dent analysis method for unidirectional laminates whose ratio of electric conductivity in each direction is 10,000.

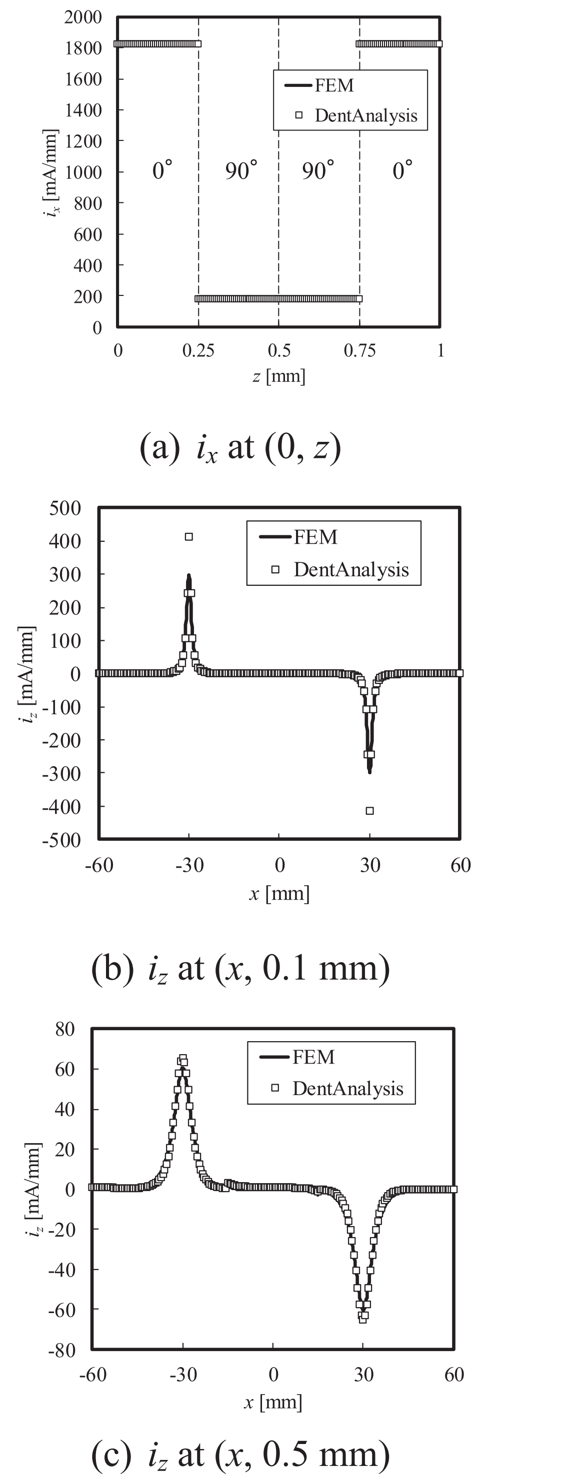

Fig. 6. Electric current density obtained by FEM and proposed dent analysis method for cross-ply laminates $[0/90]_S$ whose ratio of electric conductivity in each direction is 100.

the x direction): the abscissa is the z coordinate, and the ordinate is i_x at $x = 0$. Fig. 5(b) shows i_z (electric current density in the z direction): the abscissa is the x coordinate, and the ordinate is i_z at $z = 0.1$ mm. Fig. 5(c) shows i_z: the abscissa is the x coordinate, and the ordinate is i_z at $z = 0.5$ mm. In this calculation, $C_z = 0.00032$ was used for the equivalent conductivity.

With the increase in $\gamma = \sigma_0/\sigma_t$, the electric current distributions become complicated configurations, as shown in Fig. 5(b) and (c). The calculation results express very well the complicated distributions and agree well with the FEM results. These results indicate that the method is effective for calculating the effect of a dent for unidirectional CFRP.

3.3. Cross-ply laminate [0/90]s

Fig. 6 shows the comparison results of $\gamma = \sigma_0/\sigma_t = 100$ of the cross-ply [0/90]s specimen. Fig. 6(a) shows i_x (electric current density in the

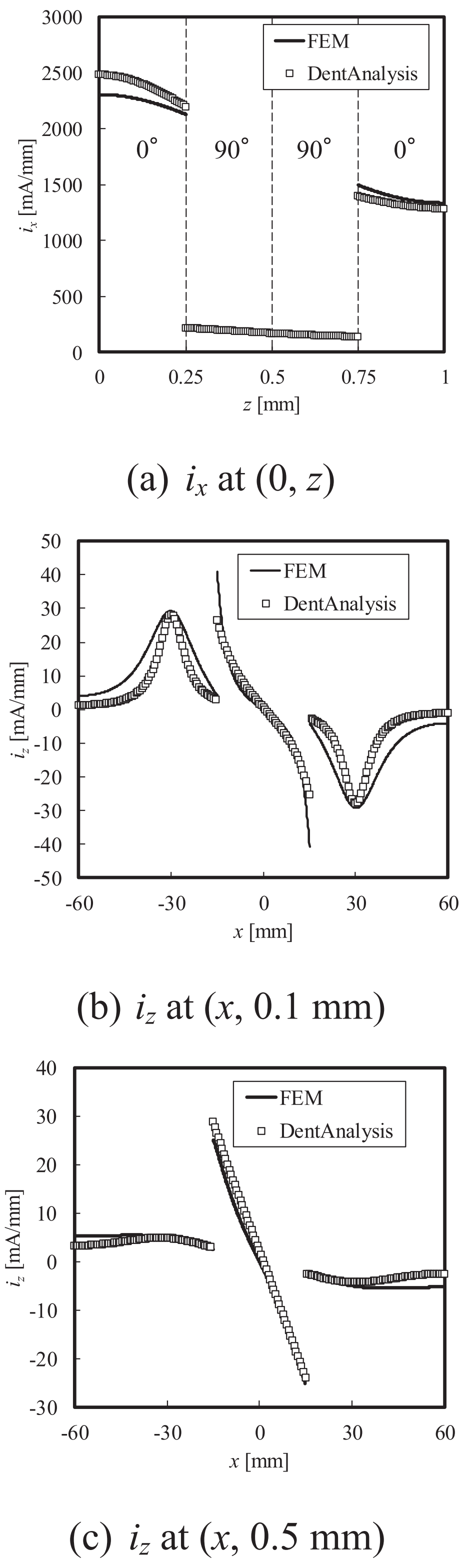

Fig. 7. Electric current density obtained by FEM and proposed dent analysis method for cross-ply laminates $[0/90]_S$ whose ratio of electric conductivity in each direction is 10,000.

x direction): the abscissa is the z coordinate, and the ordinate is i_x at $x = 0$. Fig. 6(b) shows i_z (electric current density in the z direction): the abscissa is the x coordinate, and the ordinate is i_z at $z = 0.1$ mm. Fig. 6(c) shows i_z: the abscissa is the x coordinate, and the ordinate is i_z at $z = 0.5$ mm. The solid curves are the FEM results, and the open

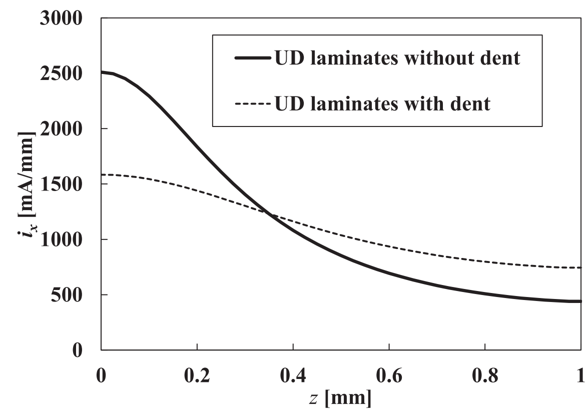

Fig. 8. Comparison of electric current density distributions between beams without a dent and with a dent.

square symbols are the results of the analysis in this study.

As described in [20], the analysis of cross-ply CFRP laminate requires the equivalent conductivity C_x, even in the x direction. This means that the analysis of the cross-ply laminate needs the equivalent conductivities C_x and C_z. Using C_x and C_z, these figures show that the calculated results agree well with the FEM results.

Fig. 7 shows the comparison results of $\gamma = \sigma_0/\sigma_t = 10{,}000$ of the cross-ply [0/90]s specimen. The electric current density distributions of the higher γ show a complicated configuration compared with the lower γ shown in Fig. 6. Especially, the i_z distributions shown in Fig. 7(b) and (c) have discontinuous curves at the dent area. The analysis method gives a good approximation of the electric current density, even in the dent area. The comparison indicates that the analysis method is useful for the estimation of the electric current density of laminated CFRPs.

3.4. Evaluation of effect of dents

Fig. 8 shows the comparison of the electric current density, i_x, distribution at of $x = 0$ and $\gamma = 10{,}000$. The abscissa is the depth from the surface, and the ordinate is the electric current density of the x direction. The solid curve shows the i_x distribution without a dent, and the dashed curve shows the i_x distribution with a dent.

The solid curve shows a high concentration of electric current at the surface. This concentration is caused by the strongly orthotropic electric current conductivity. The dashed curve is relatively smooth and flat compared with the solid curve. This means a dent results in a large electric current flow area in the through-thickness direction. This decrease in electric current concentration at the surface causes the electrical resistance to decrease. This is the reason why the generation of a dent causes an electrical resistance decrease during damage monitoring.

4. Conclusions

A calculation method to evaluate the effect of a dent on the anisotropic

electric-potential function using equivalent conductivity is proposed. The method is applied to a beam-type specimen, and the results are compared with the FEM results. The results obtained are as follows.

(1) An equivalent conductivity in the through-thickness direction is newly defined to express a local change in electric conductivity in the through-thickness direction caused by a dent.
(2) Assuming the electric-potential function of a CFRP laminate with a dent as a continuous function, an electric-potential function can be calculated for an orthotropic conductor using the equivalent conductivity.

(3) Using a beam-type specimen, the new method gives a good approximation of the electric current density distribution of a CFRP laminate with a dent.

Acknowledgment

This work was supported by AOARD FA2386-15-1-4090. The authors thank Dr. Les Lee at AFOSR for his valuable comments and suggestions.

Appendix A. Supplementary data

Supplementary data associated with this article can be found, in the online version, at http://dx.doi.org/10.1016/j.compstruct.2018.05.154.

References

[1] Schulte K, Baron Ch. Load and failure analyses of CFRP laminates by means of electrical resistively measurements. Compos Sci Tech 1989;36(1):63–76. http://dx.doi.org/10.1016/0266-3538(89)90016-X.
[2] Muto N, Yanagida H, Miyayama M, Nakatsuji T, Sugita M, Ohtsuka Y. Foreseeing of fracture in CFGFRP composites by measuring electric resistance. J Jpn Soc Compos Mater 1992;18(4):144–50. (in Japanese).
[3] Chen PW, Chung DDL. Carbon fiber reinforced concrete for smart structures capable of non-destructive flaw detection. Smart Mater Struct 1993;2(1):22–30. http://dx.doi.org/10.1088/0964-1726/2/1/004.
[4] Irving PE, Thiagarajan C. Fatigue damage characterization in carbon fibre composite materials using an electric potential technique. Smart Mater Struct 1998;7(4):456–66. http://dx.doi.org/10.1088/0964-1726/7/4/004.
[5] Abry JC, Bochard S, Chateauminois A, Salvia M, Giraud G. In situ detection of damage in CFRP laminates by electric resistance measurements. Compos Sci Tech 1999;59(6):925–35. http://dx.doi.org/10.1016/S0266-3538(98)00132-8.
[6] Seo DC, Lee JJ. Damage detection of CFRP laminates using electrical resistance measurement and neural network. Comp Struct 1999;47(1–4):525–30. http://dx.doi.org/10.1016/S0263-8223(00)00016-7.
[7] Park JB, Okabe T, Takeda N, Curtin WA. Electromechanical modelling of unidirectional CFRP composites under tensile loading condition. Compos Part A 2002;33(2). http://dx.doi.org/10.1016/S1359-835X(01)00097-5. 267e275.
[8] Ogi K, Takao Y. Characterization of piezoresistance behavior in a CFRP unidirectional laminate. Compos Sci Tech 2005;65(2):231–9. http://dx.doi.org/10.1016/j.compscitech.2004.07.005.
[9] De Baere I, Paepegem Van, Degrieck J. Electrical resistance measurement for in situ monitoring of fatigue of carbon fabric composites. Int J Fatigue 2010;32(1):197–207. http://dx.doi.org/10.1016/j.ijfatigue.2009.02.044.
[10] Selvakumaran L, Lubineau G. Electrical behaviour of laminated composites with intralaminar degradation: a comprehensive micro-meso homogenization procedure. Comp Struct 2014;108:178–88. http://dx.doi.org/10.1016/j.compstruct.2013.10.057.
[11] Todoroki A, Matsuura K, Kobayashi H. Application of electric potential method to smart composite structures for detecting delamination. JSME Int J Ser A 1995;38(4):524–30.
[12] Todoroki A, Tanaka Y, Shimamura Y. Delamination monitoring of graphite/epoxy laminated composite plate of electric resistance change method. Compos Sci Tech 2002;62(9):1151–60. http://dx.doi.org/10.1016/S0266-3538(02)00053-2.
[13] Todoroki A, Tanaka M, Shimamura Y. Measurement of orthotropic electric conductance of CFRP laminates and analysis of the effect on delamination monitoring with an electric resistance change method. Compos Sci Tech 2002;62(5):619–28. http://dx.doi.org/10.1016/S0266-3538(02)00019-2.
[14] Todoroki A, Omagari K, Shimamura Y, Kobayashi H. Matrix crack detection of CFRP using electrical resistance change with integrated surface probes. Compos Sci Tech 2006;66(11–12):1539–45. http://dx.doi.org/10.1016/j.compscitech.2005.11.029.
[15] Todoroki A, Shimazu Y, Mizitani Y. Electrical resistance reduction of laminated carbon fiber reinforced polymer by dent made by indentation without cracking. J Solid Mech Mater Eng JSME 2012;6(12):1042–52.
[16] Todoroki A, Haruyama D, Mizutani Y, Suzuki Y, Yasuoka T. Electrical resistance change of carbon/epoxy composite laminates under cyclic loading under damage initiation limit. Open J Compos Mater 2014;4(1):22–31. http://dx.doi.org/10.4236/ojcm.2014.41003.
[17] Todoroki A. Electric current analysis of CFRP using perfect fluid potential flow. Trans Jpn Soc Aeron Space Sci 2012;55(3):183–90.
[18] Todoroki A, Arai M. Simple electric-voltage-change-analysis method for delamination of thin CFRP laminates using anisotropic electric potential function. Adv Comp Mater 2014;23(3):261–73. http://dx.doi.org/10.1080/09243046.2013.851357.
[19] Yamane T, Todoroki A, Fujita H, Kawashima A, Sekine N. Electric current distribution of carbon fiber reinforced polymer beam: analysis and experimental measurements. Adv Comp Mater 2016;25(6):497–513. http://dx.doi.org/10.1080/09243046.2015.1126665.
[20] Yamane T, Todoroki A. Analysis of electric current density in carbon fiber reinforced plastic laminated plates with angled plies. Comp Struct 2017;166(15):268–76. http://dx.doi.org/10.1016/j.compstruct.2016.12.055.
[21] Matsuzaki R, Yamamoto K, Todoroki A. Crack swarm inspection for estimation of crack location in carbon fiber reinforced plastics: a numerical study. Comp Struct 2017;160(15):36–42. http://dx.doi.org/10.1016/j.compstruct.2016.10.020.